Article

Covalently tethered rhodamine voltage reporters for high speed functional imaging in brain tissue

Parker E. Deal, Pei Liu, Sarah H Al-Abdullatif, Vikram R. Muller, Kiarash Shamardani, Hillel Adesnik, and Evan W. Miller

J. Am. Chem. Soc., **Just Accepted Manuscript** • DOI: 10.1021/jacs.9b12265 • Publication Date (Web): 12 Dec 2019

Covalently tethered rhodamine voltage reporters for high speed functional imaging in brain tissue

Parker E. Deal,[‡⁂] Pei Liu,[‡⁂] Sarah H. Al-Abdullatif,[‡] Vikram R. Muller,[‡] Kiarash Shamardani,[†§] Hillel Adesnik,[†§] and Evan W. Miller[‡§†*]

Departments of [‡]Chemistry and [§]Molecular & Cell Biology and [†]Helen Wills Neuroscience Institute. University of California, Berkeley, California 94720, United States.

ABSTRACT: Voltage-sensitive fluorophores enable the direct visualization of membrane potential changes in living systems. To pair the speed and sensitivity of chemical synthesized fluorescent indicators with cell-type specific genetic methods, we here develop Rhodamine-based Voltage Reporters (RhoVR) that can be covalently tethered to genetically-encoded, self-labeling enzymes. These chemical-genetic hybrids feature a photoinduced electron transfer (PeT) triggered RhoVR voltage-sensitive indicator coupled to a chloroalkane HaloTag ligand through a long, water-soluble polyethyleneglycol (PEG) linker (RhoVR-Halos). When applied to cells, RhoVR-Halos selectively and covalently bind to surface-expressed HaloTag enzyme on genetically modified cells. RhoVR-Halos maintain high voltage sensitivities—up to 34% ΔF/F per 100 mV—and fast response times typical of untargeted RhoVRs, while gaining the selectivity typical of genetically encodable voltage indicators. We show that RhoVR-Halos can record action potentials in single trials from cultured rat hippocampal neurons and can be used in concert with green-fluorescent Ca^{2+} indicators like GCaMP to provide simultaneous voltage and Ca^{2+} imaging. In brain slice, RhoVR-Halos provide exquisite labeling of defined cells and can be imaged using epifluorescence, confocal, or two-photon microscopy. Using high-speed epifluorescence microscopy, RhoVR-Halos provide a read out of action potentials from labeled cortical neurons in rat brain slice, without the need for trial averaging. These results demonstrate the potential of hybrid chemical-genetic voltage indicators to combine the optical performance of small-molecule chromophores with the inherent selectivity of genetically-encodable systems, permitting imaging modalities inaccessible to either technique individually.

Introduction

In neurons, rapid changes in membrane potential initiate transient rises in intracellular [Ca^{2+}] and subsequent release of neurotransmitters from synaptic terminals. Capturing an overview of voltage dynamics across even small areas of the brain remains an outstanding challenge, because traditional electrode measurements of voltage are typically restricted to single cells, and the most robust imaging approach, Ca^{2+} imaging, cannot track the fast kinetics of voltage changes. Fluorescent indicators that report on voltage directly would combine the temporal resolution of voltage measurements with the spatial resolution afforded by an imaging approach.

Inspired by a theoretical description of electron transfer for imaging voltage,[1] we have been developing molecular wire-based fluorescent voltage indicators, which we hypothesize use photo-induced electron transfer (PeT)[2] as a voltage-sensing trigger. These voltage-sensitive fluorophores, or VoltageFluors, respond to changes in membrane potential with sub-microsecond response kinetics,[3-5] provide large, turn-on fluorescence responses to action potentials in neurons, and can operate with excitation wavelengths ranging from blue (VoltageFluor)[6-7] to green (Rhodamine Voltage Reporters, RhoVR)[8-9] and into the far red (Berkeley Red Sensor of Transmembrane potential, BeRST)[10] and infrared region with two photon excitation (2P).[9, 11-12] For voltage imaging with cellular resolution *in vivo*, molecular wire-based VoltageFluors possess the required speed, sensitivity, minimal invasiveness, and compatibility with 2P excitation. To date, however, the direct application of VoltageFluor-type dyes to brain slice or intact brains precludes cellular resolution of voltage dynamics – the hydrophobic nature of the molecular wire effectively targets the dyes to all membranes. Genetically encoding a voltage-sensitive fluorophore is one solution to the problem of cell-type specificity in intact brains. However, despite significant progress in developing completely genetically encoded voltage indicators (GEVIs), improvements are needed in overall brightness, localization to plasma membranes, and 2P performance. In this regard, hybrid indicators that utilize chemically-synthesized reporters in concert with genetically encoded targeting groups represent a promising route towards voltage imaging complex tissues. Indeed, the use of synthetic chemical reagents and probes in the context of neurobiology has a long[13-15] and continuing tradition.[16-22]

Scheme 1. Rhodamine Voltage Reporter-HaloTag hybrids for voltage imaging (RhoVR-Halos)

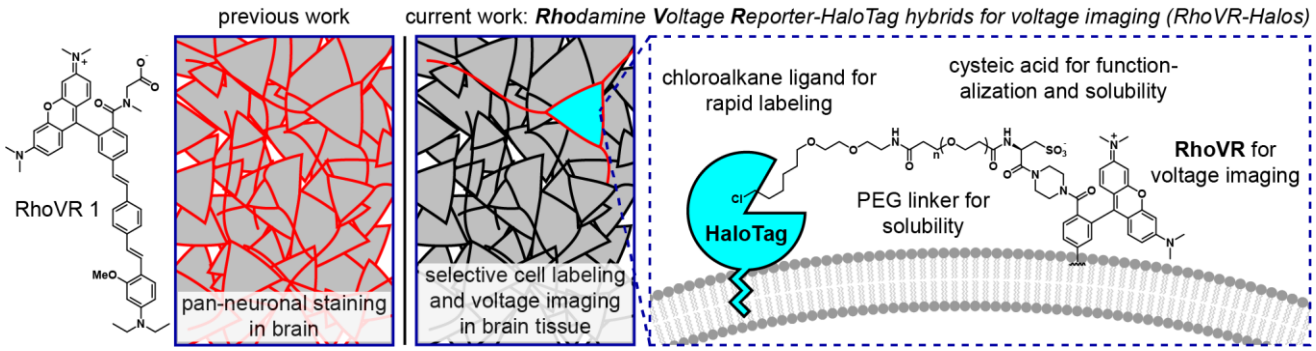

A number of strategies exist for hybrid, genetically-targeted voltage imaging. Two component hybrids rely on FRET interactions between the genetically encoded and chemical component;[23-27] whereas catalytic strategies rely on enzymatic or photochemical uncaging to either switch on fluorophores or facilitate their accumulation in plasma membranes.[28-31] More recently, covalent tethering of environmentally-sensitive dyes enabled voltage imaging in cultured neurons.[32] We were attracted to a covalent tethering approach, because it should allow us to employ the entire suite of VoltageFluors developed within our lab, rather than relying on phenol-containing fluorophores, as currently required by fluorogenic strategies developed in our lab.[29-31] In a tethering approach, the voltage-sensitive indicator is modified to include a long, flexible, water-soluble linker terminating in a ligand that forms a covalent bond with a genetically-encoded cell surface enzyme (**Scheme 1**). We recently demonstrated the feasibility of this approach by tethering VoltageFluors to the SpyTag peptide.[33] The resulting VoltageSpy compounds enable selective labeling and voltage imaging from defined neurons in culture, however improvements to labeling kinetics, 2P absorption, and voltage sensitivity are needed to afford labeling and voltage imaging in tissue.

We therefore aimed to design a tethering approach for voltage imaging using RhoVR and the HaloTag[34] self-labeling enzyme system (**Scheme 1**). RhoVR indicators provide red-shifted excitation and emission profiles,[8] high 2P cross sections,[9] large voltage sensitivities (up to 47% ΔF/F per 100 mV),[8] and a well-established synthetic route to further functionalization. In a complementary fashion, the HaloTag ligand/enzyme system[34] has been widely deployed in a number of biological contexts,[35-38] offers fast reaction kinetics[34] compared to first generation SpyCatcher,[39] and a simple synthesis to access the chloroalkane ligand. In this paper, we describe the synthesis of two new RhoVR voltage indicators that can be combined with HaloTag labeling strategies to create RhoVR-Halos. The new RhoVR-Halo indicators retain the high voltage sensitivity of their parent, untargeted indicators (>30% ΔF/F per 100 mV in HEK cells), can be combined with blue/green optical tools like GCaMP for dual voltage and Ca^{2+} imaging, and show excellent staining in immortalized cells, cultured primary neurons, and cortical neurons in brain slices. Importantly, RhoVR-Halos not only label cells, but can provide an optical readout of voltage dynamics from neurons in intact brain slices.

Results

Synthesis of piperazine-functionalized RhoVRs

Synthesis of HaloTag functionalized RhoVR 1 (RhoVR1-Halos) begins from tetramethylrhodamine voltage dye **3**, which was synthesized in 70% yield via a Heck coupling between isomerically pure Br-TMR **1** and phenylene-vinylene wire **2** (**Scheme 2**).[8] Previous studies in our lab revealed that a negatively charged functional group on the chromophore is necessary for the proper localization and function of the voltage dye.[7-8] In order to both maintain a negatively charged anchor and provide a functional handle for the attachment of the HaloTag ligand, we modified the substitution at the 2' position of our typical RhoVRs to incorporate an L-cysteic acid amino acid linker.[40] This was accomplished through a HATU mediated coupling between **3** and 1-Boc-piperazine, followed by a TFA-catalyzed deprotection of the Boc-protected amine **4** to afford **5** in 62% yield over two steps (**Scheme 2**).[24] A second HATU-mediated coupling between **5** and Boc-L-cysteic acid and subsequent TFA deprotection of the protected intermediate **6** afforded **7** in 78% yield over two steps.

Compound **7** possesses absorption and emission properties similar to the parent RhoVR 1,[8] with a λ_{max} at 565 nm (ε = 82,000 $M^{-1}cm^{-1}$) and emission maximum at 585 nm (**Table 1**, **Figure 1a**). In HEK293T cells, **7** localizes to plasma membranes (**Figure 1b-c**). The effective cellular brightness of **7** was lower than that of RhoVR 1, when both dyes were loaded at the same concentration (**Figure S1**, **Table 1**). Compound **7** is voltage-sensitive. Simultaneous fluorescence imaging and patch-clamp electrophysiology in HEK293T cells stained with 500 nM **7** reveals a voltage sensitivity of approximately 38% ΔF/F per 100 mV (**Table 1**, **Figure 1d-e**). This value is slightly lower than RhoVR 1 (47% ΔF/F per 100 mV, **Table 1**).

Synthesis of RhoVR1-PEG$_x$-Halos

Due to the covalent nature of HaloTag labeling, we hypothesized that a long linker might be required to allow the tethered RhoVR to properly insert into the plasma membrane while bound to the active site of HaloTag. We

Scheme 2. Synthesis of piperazine-cysteic acid functionalized RhoVR 7

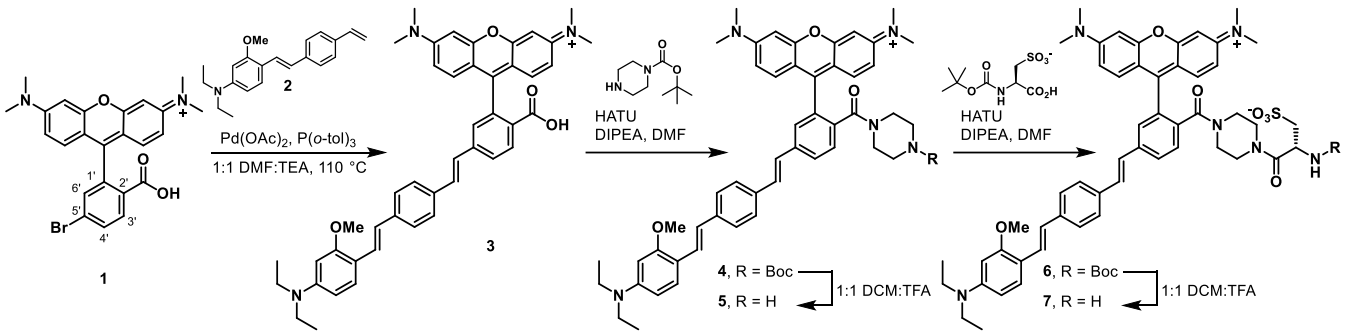

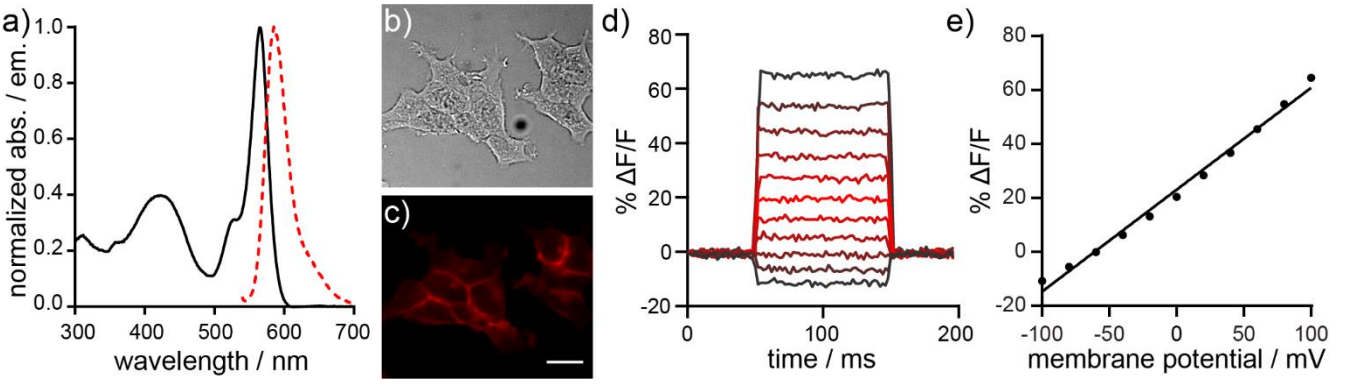

Figure 1. Characterization of RhoVR **7**. **a)** Normalized absorption and emission spectra for **7**. Spectra were obtained in Dulbecco's phosphate buffered saline (dPBS) with 0.1% SDS. Dye concentration was 500 nM. **b)** Transmitted light (DIC) and **c)** widefield fluorescence microscopy image of HEK293T cells stained with **7**. Dye was loaded for 30 min at 37 °C. Scale bar is 20 µm. **d)** Plot of fractional change in fluorescence (ΔF/F) vs time for a single HEK293T cell stained with **7** and subjected to 100 ms hyper- and depolarizing steps (±100 mV, 20 mV increments) from a holding potential of -60 mV under whole-cell voltage-clamp mode. **e)** A plot of fractional change in fluorescence (ΔF/F) vs. final membrane potential (mV). Data depict mean ΔF/F ± standard deviation (error bars are smaller than markers) for n = 4 individual cells loaded with **7**.

therefore synthesized a library of RhoVR1-PEG$_x$-Halo derivatives with varying lengths of PEG linkers in order to determine the effect of linker length on voltage sensitivity. From **7**, NHS-ester activated dPEG® linkers with either 5, 9, 13, or 25 ethylene monomer units (spanning a theoretical linear distance of about 21 to 92 Å) were coupled to the free amine of the L-cysteic acid moiety of **7** (**Scheme 3**). Subsequent HATU-mediated coupling of the HaloTag-amine ligand and purification by preparative HPLC afforded RhoVR1-PEG$_x$-Halo dyes **12** – **15** in 24-53% yield; x = the number of ethylene glycol monomer units (x = 5, **12**; x = 9, **13**, x = 13, **14**; x = 25, **15**). We also synthesized a "PEG$_o$" RhoVR1-Halo derivative **16** using a succinic anhydride-derived linker (**Scheme S1**). The absorption and emission properties of the new RhoVR1-PEG$_x$-Halo compounds matched those of **7** (**Figure S2**).

Design of cell-surface expressed HaloTag enzymes

In order to express the HaloTag enzyme on the cell surface, we fused a transmembrane domain (pDisplay) derived from platelet-derived growth factor receptor (PDGFR)[41-42] or a glycophosphatidyl inositol (GPI) signal peptide derived from decay accelerating factor (DAF)[43] to the C-terminal of the HaloTag sequence. We also appended a secretion signal peptide from immunoglobulin K (IgK) to the N-terminal to enhance extracellular trafficking (**Figure S3a**). To track the protein expression in live cells, we included a nuclear-localized EGFP downstream of HaloTag, separated by an internal ribosome entry site (IRES). We tested the effectiveness of the pDisplay and DAF constructs in live HEK293T cells using a cell-impermeant tetramethylrodamine (TMR)-Halo ligand **44** (**Scheme S2**). Bath application of TMR-Halo **44** at 50 nM for 30 minutes showed clear membrane-bound fluorescence, which matched EGFP signal in transfected cells (**Figure S3b-e**). In HEK293T cells, use of pDisplay-based constructs results in marginally higher RhoVR fluorescence than the analogous DAF constructs (**Figure S4a-b**); therefore, we used pDisplay-enabled targeting for all future studies.

Cellular characterization of RhoVR1-PEG$_x$-Halos

RhoVR1-PEG$_x$-Halo compounds selectively label HEK293T cells that express cell-surface HaloTag enzyme (**Figure 2a-d**, **Figure S4c-d**, **Figure S5a-d**). RhoVR fluorescence depends on expression of HaloTag; higher levels of HaloTag enzyme, estimated by higher EGFP fluorescence intensity, correlates with high RhoVR fluorescence (**Figure S4e**). Selective labeling can be achieved in as little as 5 minutes (50 nM **15**), and staining improved with longer incubation times (we examined up to 30 min loading times, **Figure S4f**). Selective labeling appeared independent of reaction temperature. Both 37 °C and 22 °C loading temperature gave similar cellular RhoVR fluorescence values (**Figure S4g**). We observed effective RhoVR staining

Scheme 3. Synthesis of RhoVR1-Halos

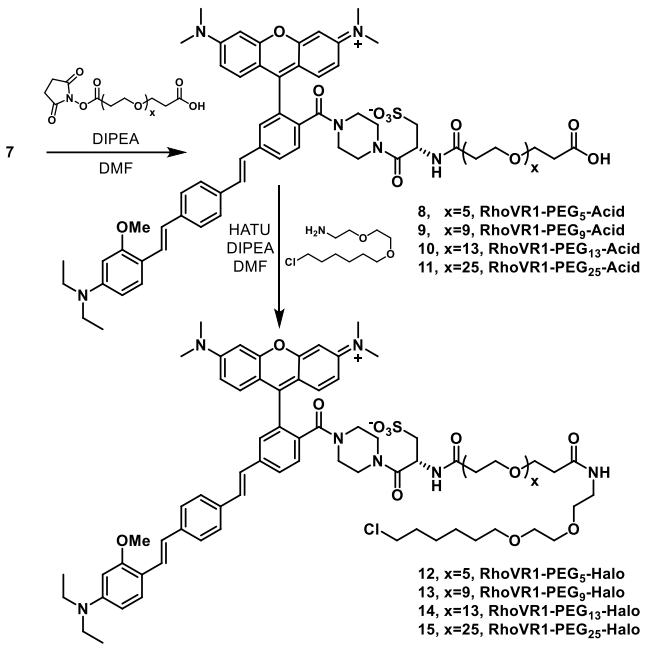

at concentrations as low as 5 nM, indicating the fast kinetics of HaloTag labeling leads to rapid sequestration of the dye.[21] Although the contrast ratio decreases, we still observe highly selective labeling at concentrations as high as 500 nM (**Figure S4c-d**). We hypothesize the minimal off-target labeling is due to the increased water solubility of RhoVR1-PEG$_x$-Halos afforded by the L-cysteic acid and PEG linkers.[23]

Voltage sensitivity of RhoVR-PEG$_x$-Halos

Possessing a library of RhoVR-PEG$_x$-Halo compounds allowed us to examine the relationship between tether length and voltage sensitivity. RhoVR1-PEG$_0$-Halo **16**, which incorporates a very short succinic anhydride-derived linker, shows no voltage sensitivity in HaloTag-expressing HEK293T cells (**Figure S6a-c**, **Table 1**), despite displaying selective labeling in these same cells (**Figure S5a**). We hypothesize that the short linker of **16** prevents the RhoVR component of the molecule from inserting into the plasma membrane when the chloroalkane tail of **16** is ligated in the active site of the HaloTag enzyme. Increasing PEG linker length improves the voltage sensitivity of RhoVR1-PEG$_x$-Halo compounds. Voltage sensitivity increases from 0% (**16**, **Figure S6a-c**) to 11% ΔF/F per 100 mV for **12**, which possesses a PEG$_5$ linker of about 21 Å (**Figure S6d-f**, **Table 1**). Longer PEG linkers are even more voltage sensitive, 20% for **13** (PEG$_9$, ~35 Å, **Figure S6g-i**), 26% for **14** (PEG$_{13}$, ~50 Å, **Figure S6j-l**), and 34% for **15** (PEG$_{25}$, ~92 Å, **Figure S6m-o**). At 34% ΔF/F per 100 mV, RhoVR1-PEG$_{25}$-Halo **15** nearly recovers the full voltage sensitivity of the parent RhoVR (38%, **7**). The linker length dependence on the voltage sensitivity of RhoVR-Halos contrasts with previous results from our lab.[33] We found no dependence on PEG linker length for fluorescein-based voltage indicators targeted via similar covalent tethering through

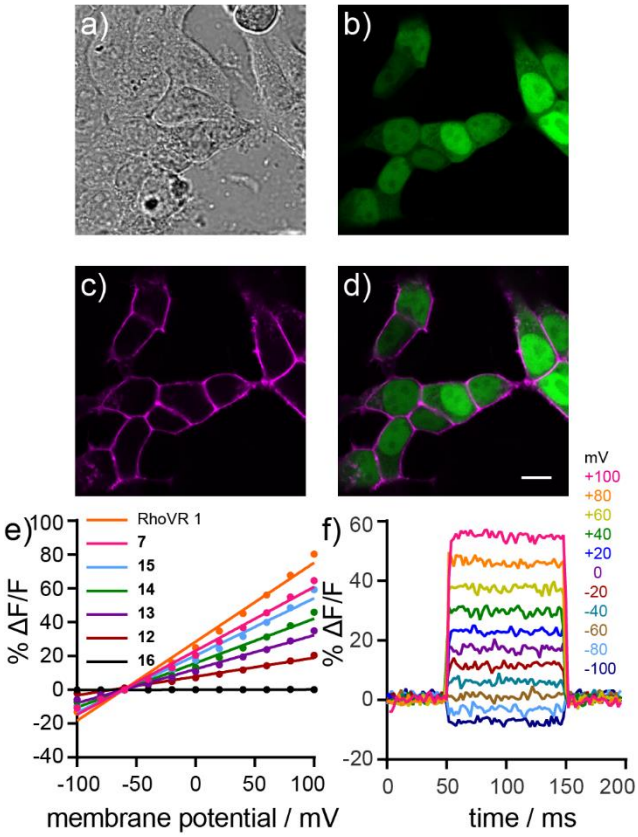

Figure 2. Cellular labeling and voltage sensitivity of RhoVR1-PEG$_x$-Halo compounds. **a)** DIC image of HEK293T cells expressing nuclear EGFP stained with **15**. **b)** Confocal fluorescence image of HaloTag expressing cells from **(a)** as indicated by nuclear EGFP fluorescence. **c)** Confocal fluorescence image showing the fluorescence of **15** from cells in **(a)**. **d)** Merge of fluorescence from EGFP (green) and **15** (magenta), demonstrating the highly selective localization of **15** to HaloTag expressing cells. Scale bar is 10 μm. **e)** Plot of % ΔF/F vs final membrane potential for RhoVR 1, **7** and RhoVR1-PEG$_x$-Halo derivatives **12-16** (n=3-9, error bars not shown). **f)** Plot of the fractional change in fluorescence of **15** vs time for 100 ms hyper- and depolarizing steps (±100 mV in 20 mV increments) from a holding potential of -60 mV for single HEK293T cells under whole-cell voltage clamp mode.

SpyTag/SpyCatcher interactions.[33] The larger size of HaloTag (~33 kDa) vs. SpyCatcher (~15 kDa) may require longer linkers to allow proper insertion and orientation of RhoVRs into the plasma membrane.

RhoVR(Me) and brighter RhoVR(Me)-PEG$_x$-Halos

One potential limitation to the covalent labeling strategy is that the brightness of RhoVR fluorescence on the membrane is dependent on the number of enzymes displayed on the cell surface (**Figure S4e**). Loading screens showed that RhoVR1-PEG$_x$-Halo compounds were 3-4 fold dimmer than bath applied RhoVR 1 under normal loading conditions (**Figure S5**, **Table 1**). In attempt to address this limitation, we synthesized a new RhoVR derivative, dubbed RhoVR(Me), which includes a methyl-substituted molecular wire as opposed to the methoxy-substituted wire of RhoVR 1 (**Scheme S3**). We hypothesized that decreasing the electron-donating nature of the aniline substitution

Table 1. Properties of RhoVR and RhoVR-Halo Tag Compounds

RhoVR-Halo Derivative	ε_{565}[a] M^{-1} cm^{-1}	Φ_{Fl}	$\Delta F/F$[c] (100 mV)	Rel. Brightness[c]	SNR[c] (100 mV)
RhoVR 1 (500 nM)	87,000	0.045[a]	47%	100%	90
7	82,000	0.026[a]	38%	18%	30
RhoVR1-PEG_{25}-Halo, **15**	74,000	0.050[a], 0.017[b]	34%	30%	34
RhoVR1-PEG_{13}-Halo, **14**	-	-	26%	29%	30
RhoVR1-PEG_{9}-Halo, **13**	-	-	20%	34%	14
RhoVR1-PEG_{5}-Halo, **12**	-	-	11%	32%	11
RhoVR1-PEG_{0}-Halo, **16**	-	-	0%	61%	-
RhoVR(Me) (500 nM), **21**	81,000	0.022[a]	13%	220%	77
RhoVR(Me)-PEG_{25}-Halo, **27**	85,000	0.038[a], 0.009[b]	16%	118%	40
RhoVR(0), **32**	71,000	0.219[a]	0%	-	-
RhoVR(0)-PEG_{25}-Halo, **38**	83,000	0.214[a]	0%	-	-

[a] PBS, pH 7.2, 0.1% SDS [b] HBSS [c] voltage-clamped HEK cells

might increase the molecular brightness of RhoVR(Me) compared to RhoVR1, owing to less electron-donating ability of methyl compared to methoxy.

The synthesis of the untargeted RhoVR(Me) was analogous to RhoVR 1, starting with a Heck coupling between isomerically pure Br-TMR **1** and phenylenevinylene wire **18** to generate voltage dye **19** in 80% yield. Formation of an N-methyl glycine-derived tertiary amide at the 2' position of the pendant aryl ring gave the untargeted RhoVR(Me) **21** in 77% yield over two steps (**Scheme S3**). The absorption and emission spectra of RhoVR(Me) is nearly identical to that of RhoVR 1 and **7** (**Figure S2b**, **Table 1**). Like RhoVR 1 and **7**, RhoVR(Me) (**21**) localizes to the plasma membranes of HEK293T cells (**Figure S7a-b**). RhoVR(Me) is approximately 4-fold brighter than RhoVR 1, under identical loading conditions (**Figure S5**, **Table 1**). Patch-clamp electrophysiology revealed the increased brightness came at the cost of voltage sensitivity, with RhoVR(Me) possessing a lower 13% ΔF/F per 100 mV (**Figure S7c-d**, **Table 1**). When accounting for both the cellular brightness and voltage sensitivity of the dyes, the signal to noise ratio (SNR) of RhoVR(Me) (77:1) is close to RhoVR 1 (80:1) and better than **7** (30:1). In particular, RhoVR(Me) may be a promising indicator when the photon budget is a limiting factor for imaging.

RhoVR(Me)-PEG_{25}-Halo synthesis and cellular characterization

Genetically-targeted versions of RhoVR(Me) can be readily synthesized by adapting the methods for generating RhoVR1-Halos **12** – **15**. RhoVR(Me) precursor **19** can be converted to the piperazine/L-cysteic acid-functionalized **25** in two steps (**Scheme S4**). Coupling of the NHS-ester activated NHS-PEG_{25}-acid linker followed by HATU-mediated coupling of HaloTag-amine affords RhoVR(Me)-PEG_{25}-Halo **27** in 28% yield over two steps. Compound **27** selectively stains HEK293T cells expressing HaloTag (**Figure S7e-h**). Patch-clamp electrophysiology in HEK293T cells reveals that **27** had a voltage sensitivity of 16% ΔF/F per 100 mV, similar to the parent, untargeted RhoVR(Me) (**Figure S7i-j**, **Table 1**). RhoVR(Me)-PEG_{25}-Halo **27** was 3-4 fold brighter than RhoVR1-PEG_{25}-Halo **15** in HEK cells (**Table 1**). This recapitulates results with the untargeted dyes (**Figure S5**). Because total dye concentration in the membrane is correlated to the number of HaloTag enzymes, this result suggests that the increased brightness of RhoVR(Me) over RhoVR 1 is due to reduced PeT quenching, and not because of improved uptake of RhoVR(Me) into the plasma membrane.

We also synthesized two voltage-insensitive RhoVR compounds as controls. RhoVR(0), **32**, possesses a sarcosine-amide membrane anchor but lacks an aniline substitution on the molecular wire (**Scheme S5**). Although **32** possesses absorption and emission spectra similar to RhoVR1 (**Figure S2c**) and localizes to cellular membranes (**Figure S7e-f**), it is not voltage-sensitive (**Figure S7g-h**), consistent with a PeT-based mechanism of voltage sensing. In a similar fashion, we also synthesized a piperazine-cysteic acid functionalized RhoVR(0) (**36**) and coupled it to the HaloTag ligand via a PEG_{25} spacer (**Scheme S6**). Just like the untargeted indicators, RhoVR(0)-PEG_{25}-Halo (**38**) has a higher quantum yield than RhoVR1-PEG_{25}-Halo (**15**), but is not voltage sensitive (**Table 1**).

*Characterization of RhoVR1-PEG_{25}-Halo **15** and RhoVR(Me)-PEG_x-Halo **27** in neurons*

Having established the selective staining and voltage sensitivity of both **15** and **27** in HEK293T cells, we next evaluated these hybrid chemical-genetic indicators in cultured rat hippocampal neurons. The plasmids encoding HaloTag constructs were modified by replacing the CMV promoter with a neuron-specific synapsin promoter. A regulatory element from the woodchuck hepatitis virus (WPRE) was also added to improve protein expression (**Figure S3a**). In neurons, membrane targeting with either DAF or the single-pass transmembrane domain of pDisplay appeared equally effective (**Figure S8**); however, since pDisplay gave the best results in HEK293T cells, we continued with its use in neurons.

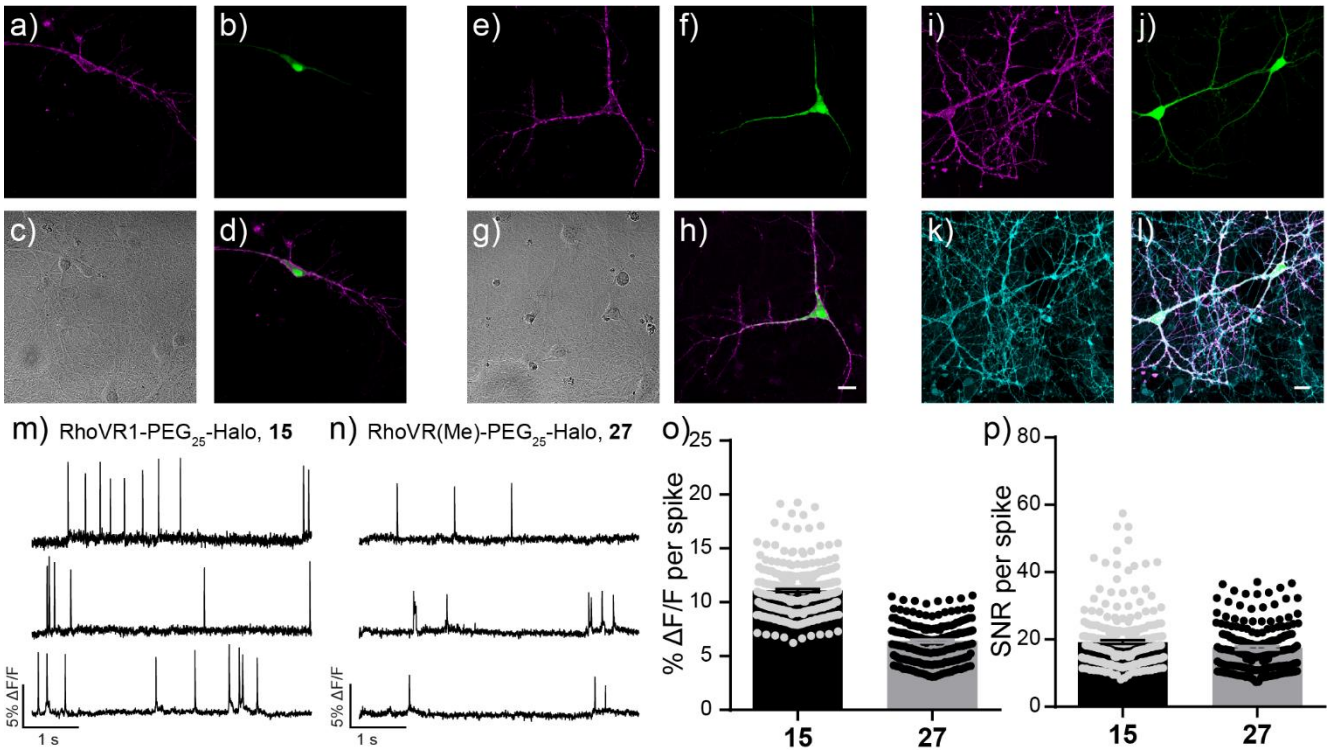

Figure 3. Evaluation of RhoVR-Halos **15** and **27** in cultured rat hippocampal neurons. Confocal fluorescence microscopy images (single optical section of ~0.8 μm) depicting the selective labeling of HaloTag expressing neurons with (**a-d**) **15** or (**e-h**) **27**. **a** and **e**) RhoVR fluorescence is localized to the plasma membrane of the HaloTag expressing neurons. **b** and **f**) EGFP fluorescence indicates expression of HaloTag (pDisplay). **c** and **g**) DIC image and **d** and **h**) merged image of neurons in panels (**a**/**b**) and (**e**/**f**). Scale bar is 20 μm. **i**) Maximum projection of RhoVR-Halo **27** fluorescence in **j**) HaloTag and EGFP-expressing neurons. **k**) Counterstaining with silicon-rhodamine BeRST reveals pan-membrane staining. **l**) Merged image showing RhoVR (magenta), EGFP (green), and BeRST (cyan) fluorescence. Scale bar is 20 μm. Plots of fractional change in fluorescence (ΔF/F) vs time in hippocampal neurons stained with **m**) **15** or **n**) **27**. **o**) Average ΔF/F and **p**) SNR per spike for evoked action potentials recorded with RhoVR-Halos. Error bars are ±S.E.M. for n = 256 or 186 spikes from 30 or 21 neurons for RhoVR1-PEG$_{25}$-Halo (**15**) or RhoVR(Me)-PEG$_{25}$-Halo (**27**), respectively.

Sparsely transfected neurons were stained with either **15** or **27** at 50 nM. Similar to HEK293T cells, both dyes labeled HaloTag expressing neurons with high selectivity (**Figure 3**). Both **15** (**Figure 3a**) and **27** (**Figure 3e**) clearly label the cell bodies and processes of neurons expressing HaloTag/GFP (**Figure 3b** and **f**). The exquisite labeling of chemical-genetic methods like RhoVR(Me)-PEG$_{25}$-Halo **27** is highlighted by comparing to simultaneous loading with the untargeted, far-red indicator, BeRST[10] (**Figure 3i-l**). While BeRST stains all cellular membranes (**Figure 3k**), RhoVR(Me) fluorescence (**Figure 3i**) is limited to the neuron expressing HaloTag (**Figure 3j**). Both **15** and **27** can report on voltage dynamics in cultured neurons that express HaloTag. Spontaneously firing action potentials were detected with an average ΔF/F of 11.1 ± 0.1% (N = 256 spikes, 30 neurons) for **15** and 6.4 ± 0.1% (N = 186 spikes, 21 neurons) for **27**. Patch clamp electrophysiology in cultured neurons, along with neurons expressing HaloTag alone or expressing HaloTag and labeled with RhoVR1-PEG$_{25}$-Halo **15**, demonstrates that **15** has little impact on the membrane properties of neurons. This includes resting membrane potential, action potential kinetics, and membrane capacitance (**Figure S9**). Expression of HaloTag (but not addition of RhoVR compounds) caused a small, but statistically significant, decrease on membrane capacitance (**Figure S9a**).

Comparison of RhoVR1-PEG$_{25}$-Halo to genetically-encoded voltage indicators

We compared the performance of **15** to the commonly used genetically-encoded voltage indicators ASAP2f,[44] based on circularly permuted green fluorescent protein (cpGFP), and Ace2N-mNeon (Ace2N),[12] which uses the mNeon fluorescent protein[45] appended to the *Acetabularia acetabulum* rhodopsin (Ace) voltage sensitive domain. Neurons labeled with **15** compared favorably to both ASAP2f and Ace2N expressing neurons, displaying brighter and red-shifted membrane fluorescence at matched light powers (**Figure S10**), turn-on responses to action potentials (ASAP2f and Ace2N-mNeon both possess turn-off responses) (**Figure S10a**) and an average ΔF/F per spike of 10.4% ± 0.2% (SNR= 16.5:1) for evoked action potentials, compared to -4.4% ± 0.1% (SNR= 9:1) per spike for ASAP2f and -1.8% ± 0.1% per spike for Ace2N (SNR= 16.7:1) (**Figure S10b-c**). Another advantage of our chemical-genetic tethering approach is greatly improved membrane localization of fluorescence. Because the genetically encoded HaloTag

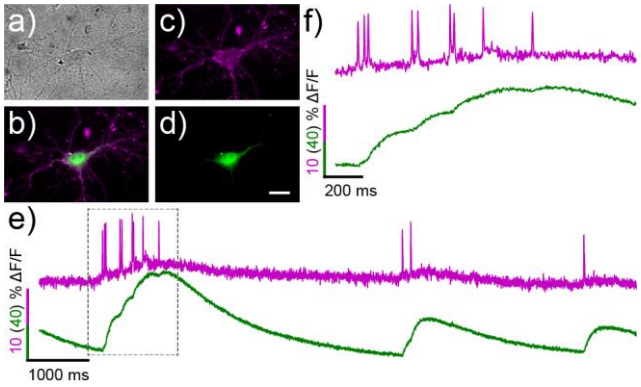

Figure 4. Simultaneous, two-color voltage and Ca^{2+} imaging in hippocampal neurons with RhoVR-Halo **15** and GCaMP6s. **a**) Transmitted light image of neurons expressing cell-surface HaloTag and cytosolic GCaMP6s. **b**) Merged widefield fluorescence microscopy image depicting **15** (magenta) and GCaMP6s (green) staining. Individual channels of the same neuron show **c**) membrane-associated **15** and **d**) cytosolic GCaMP6s. **e**) Plot of ΔF/F vs time for **15** (magenta) and GCaMP6s (green). **f**) Expanded time scale of the boxed region in panel **(e)**. Scale bar is 20 μm.

protein is non-fluorescent and the RhoVR-Halo dye is impermeable to the plasma membrane, we only observe RhoVR staining when both components are present at the cell surface (**Figure S4, S8**). In contrast, GEVIs rely on genetically encoded fluorescent proteins that can contribute high amounts of unresponsive background fluorescence during the various stages of their assembly/export to the plasma membrane (**Figure S10d-e**).

Dual voltage and Ca^{2+} imaging with RhoVR1-PEG$_{25}$-Halo and GCaMP6s

Since the red-shifted absorbance/emission profile of RhoVR-Halos allows their use alongside green fluorescent tools, we demonstrated our ability to carry out dual-color calcium and voltage imaging in genetically defined cells by replacing the nuclear EGFP marker with a genetically encode calcium sensor GCaMP6s (**Figure S3**).[26] Neurons expressing the HaloTag-GCaMP6s construct were selectively labeled with **15** with the same efficiency as the HaloTag-EGFP constructs (**Figure 4**). Simultaneous excitation with both blue and green light and segregation of the resulting emission into RhoVR-Halo and GCaMP6s fluorescence channels allowed us to visualize both the rapid changes in membrane potential and the corresponding slower increase in [Ca^{2+}] during spontaneous spiking events (**Figure 4**). The sensitivity of **15** to these action potentials was similar to those obtained at a single wavelength (ΔF/F per spike = 5.3 ± 0.9%, SNR = 15.6:1, N = 18 spikes). RhoVR and GCaMP6s fluorescence emission are well separated; even when large Ca^{2+} spikes are recorded with GCaMP6 (**Figure S11a** and **e**), RhoVR fluorescence remains uncontaminated (**Figure S11e**) by bleed-through from GCaMP6s. In all cases, the fast voltage spike precedes the subsequent Ca^{2+} transient.

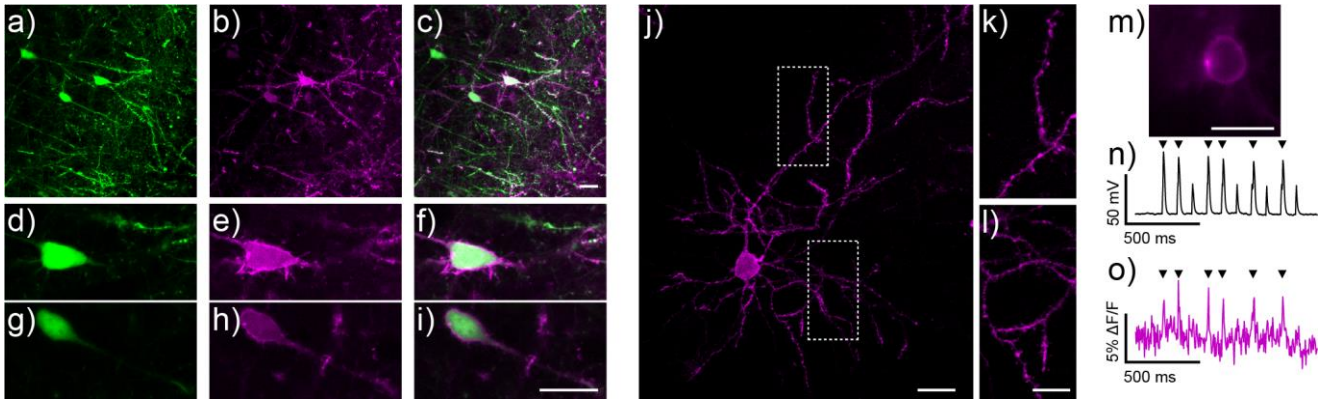

Figure 5. Brain slice imaging with RhoVR1-PEG$_{25}$-Halo **15** under widefield, one-photon confocal, and two-photon microscopy. **a-i**) One-photon, confocal microscopy of **15** in mouse brain slice prepped from animals expressing HaloTag-pDisplay and EGFP (introduced via *in utero* electroporation). Maximum projection of **a**) EGFP (green), **b**) **15** (magenta), and **c**) merged fluorescence in mouse cortical brain slice stained with **15** (250 nM, 15 min loading). Maximum projections are constructed from 25 slices with optical sections of about 0.8 μm. **d-i**) Zoomed-in, single optical slice confocal images of cells from panels (**a-c**). **d** and **g**) EGFP-associated fluorescence. **e** and **h**) RhoVR-associated fluorescence. **f** and **i**) Overlay of EGFP (green) and **15**(magenta) fluorescence. Scale bar is 20 μm. **j-k**) Two photon microscopy of **15** in cortical brain slice prepared from a mouse expressing pDisplay-HaloTag (*in utero* electroporation). **j**) RhoVR fluorescence associated with a slice treated with 250 nM **15** for 15 min at room temperature. Image is a maximum projection of 100 optical slices over 37 μm, with excitation provided at 860 nm. Scale bar is 20 μm. **k** and **l**) Expanded view of boxed regions in panel (**j**). Scale bar is 10 μm. **m-o**) Widefield fluorescence microscopy and dual voltage imaging and electrophysiology of cortical neurons in brain slice stained with **15**. **m**) Widefield fluorescence image of **15** fluorescence (250 nM, 15 min loading) in a cortical neuron expressing HaloTag-pDisplay. **n**) Plot of voltage vs. time for the neuron in panel (**n**) during current injection to evoke action potentials. Electrophysiology is digitized at 20 kHz. **o**) Plot of ΔF/F vs. time for the same neuron. Fluorescence data was acquired at 500 Hz, and is not corrected for bleaching. Arrows indicate evoked spike. Small spike are sub-threshold current injections. Scale bar is 20 μm.

Because of the fast kinetics of V_m compared to Ca^{2+} transients, monitoring V_m directly enables better resolution of spike timing than Ca^{2+}, especially when spikes occur in quick succession.

Deploying RhoVRs in mouse brain slice

Inspired by the performance of RhoVR-Halos in cultured cells,we applied our chemical-genetic labeling strategy to brain tissue samples. We prepared brain slices from mice expressing cell-surface HaloTag (pDisplay). The gene for HaloTag was introduced by *in utero* electroporation of a mixture of HaloTag-pDisplay under control of the synapsin promoter and either pCAG-EGFP or pCAG-mTagBFP2 as a marker for expression in slice preparation. Approximately 300 μm-thick coronal slices were loaded with 250 nM RhoVR1-PEG_{25}-HaloTag **15** at room temperature for 15 min and imaged via confocal microscopy (**Figure 5a-i**).

In contrast to the non-specific staining we observe with untargeted dyes (**Figure S12**), application of **15** to brain slices expressing cell-surface HaloTag provides cell-specific labeling in the sparsely labeled EGFP cells found in layer 2/3 of the cortex (**Figure 5a-i**). RhoVR fluorescence (**Figure 5b,e,h**) from cell bodies and processes is clearly visible and correlates with EGFP fluorescence (**Figure 5a,d,g**). Not all EGFP-positive cells display RhoVR fluorescence, which we hypothesize is a result of introducing the EGFP marker on a separate plasmid during *in utero* electroporation. Confocal microscopy reveals strong RhoVR **15** fluorescence down to 50 μm below the surface (**Figure S13**). **15** can be readily observed from single cells as deep as 100 μm below the surface of the slice, indicating good penetration during the 15-minute loading period (**Figure S13**). Staining near the surface of the brain slice does not appear selective (**Figure S13**), which we hypothesize is due to both the tendency of damaged tissues at the cut site of the slice to take up dyes and to saturation of any membrane-bound HaloTag enzymes.

The high two-photon cross section of rhodamine dyes allows RhoVR1 and related compounds[9, 12] to be imaged under two-photon illumination. We generated a normalized two-photon absorption cross section (GM) plot of **15** and **27** (**Figure S14**). RhoVR **15** and **27** have two-photon cross section maxima near 830 nm, in good agreement with the reported maxima for related rhodamine compounds (**Figure S4a**).[9] Both RhoVRs possess reasonable absorption cross sections at around 1030 – 1040 nm, making them useful for newly developed kHz-rate two-photon microscopies that require excitation near this wavelength.[12] Two-photon microscopy of **15** reveals excellent staining of single neurons in layer 2/3 of the cortex (**Figure 5j-l**); both neuronal soma (**Figure 5j**) and processes are clearly visible when excited at 860 nm (**Figure 5k,l**). Illumination with 920 nm and 1040 nm also provides clear visualization of **15**labeled neurons (**Figure S14b-c**)

RhoVR1-PEG_{25}-Halo 15 is voltage-sensitive in brain slice. We performed dual optical and electrophysiological recordings from whole-cell, patch-clamped neurons in cortical layer 2/3 of mouse brain slices. We evoked a train of action potentials in the RhoVR-stained neuron (**Figure 5m**) via current injection and recorded the responses both electrophysiologically (**Figure 5n**) and optically (**Figure 5o**). RhoVR1-PEG_{25}-Halo **15** clearly records action potentials in a single trial (indicated by black arrows), with an average ΔF/F per spike of 4.3% (± 0.3% S.E.M. for n = 6 spikes) and SNR of approximately 3.3 (± 0.6, S.E.M. for n = 6 spikes).

Discussion

We present the design, synthesis, and application of genetically targetable tetramethylrhodamine voltage indicators (RhoVR-Halos) that combine the specificity of self-labeling proteins[39, 46-51] with the favorable photophysics of small-molecule Rhodamine Voltage Reporters. RhoVR-Halos label HaloTag expressing cells and neurons with exceptional selectivity (≥30-fold selectivity over untransfected neurons in culture) and record membrane potential changes with high sensitivities (up to 34% ± 2% ΔF/F per 100 mV in HEK cells, 6.7% ± 0.2% ΔF/F per spike in cultured neurons, and 4.3% ± 0.3% per spike for neurons in slice). We demonstrated the utility of RhoVR-Halos for simultaneous dual-color imaging, for example enabling simultaneous V_m and Ca^{2+}, and their compatibility with 2P excitation. Finally, we demonstrated the ability to selectively label individual neurons and record neuronal activity in brain slice with RhoVR-Halos, a feat not previously possible with RhoVRs or other molecular wire-based chemical indicators.

Taken together, these results demonstrate the power of a chemical/genetic voltage indicator to combine the favorable photophysics—excitation and emission profiles beyond GFP, excellent voltage sensitivity, compatibility with two-photon excitation, turn-on response to action potentials, and nanosecond response kinetics[4]—of molecular-wire based indicators with the selectivity afforded to genetically encoded proteins. Due to the modularity of this approach, we envision deploying RhoVR-Halos alongside orthogonal hybrid reporters developed in our lab (like VoltageSpy) as well as applying this chemical genetic approach to other molecular wire-based indicators, like carboVF and BeRST. Additionally, RhoVR-Halo is unique in its ability to function as a hybrid chemical-genetic voltage indicator with turn-on responses and large two-photon cross sections. This, combined with emerging holographic and kilohertz framerate two photon methodologies,[12] make RhoVR-Halos promising candidates for interrogating voltage dynamics in the context of intact brains.

ASSOCIATED CONTENT

Supporting Information. Supplementary data, including supporting figures, spectra, procedures, and analysis. This material is available free of charge via the Internet at http://pubs.acs.org.

AUTHOR INFORMATION

Corresponding Author

* Evan W. Miller, evanwmiller@berkeley.edu
⁂ These authors contributed equally.

ACKNOWLEDGMENT

Research in the Miller lab is supported by grants from the NIH (R01NS098088, R35GM119855) and Klingenstein-Simon Foundations (40746). E.W.M and H.A. acknowledge support from NSF Neuronex (1707350). 900 MHz NMR were acquired at the Central California 900 MHz NMR Facility, supported by NIH grant GM68933. UC Berkeley, HRMS data was collected at the QB3/Chemistry Mass Spectrometry Facility (Berkeley) with the assistance of Dr. Ulla N. Andersen. Confocal and 2-photon imaging experiments were performed at the CRL Molecular Imaging Center, supported by the Helen Wills Neuroscience Institute.

REFERENCES

1. Li, L.-s., Fluorescence Probes for Membrane Potentials Based on Mesoscopic Electron Transfer. *Nano Letters* **2007,** *7* (10), 2981-2986.

2. de Silva, A. P.; Gunaratne, H. Q. N.; Habib-Jiwan, J.-L.; McCoy, C. P.; Rice, T. E.; Soumillion, J.-P., New Fluorescent Model Compounds for the Study of Photoinduced Electron Transfer: The Influence of a Molecular Electric Field in the Excited State. *Angewandte Chemie International Edition in English* **1995,** *34* (16), 1728-1731.

3. Miller, E. W.; Lin, J. Y.; Frady, E. P.; Steinbach, P. A.; Kristan, W. B.; Tsien, R. Y., Optically monitoring voltage in neurons by photo-induced electron transfer through molecular wires. *Proceedings of the National Academy of Sciences* **2012,** *109* (6), 2114-2119.

4. Beier, H. T.; Roth, C. C.; Bixler, J. N.; Sedelnikova, A. V.; Ibey, B. L., Visualization of Dynamic Sub-microsecond Changes in Membrane Potential. *Biophysical Journal* **2019,** *116* (1), 120-126.

5. Lazzari-Dean, J. R.; Gest, A. M. M.; Miller, E. W., Optical estimation of absolute membrane potential using fluorescence lifetime imaging. *eLife* **2019,** *8*, e44522.

6. Woodford, C. R.; Frady, E. P.; Smith, R. S.; Morey, B.; Canzi, G.; Palida, S. F.; Araneda, R. C.; Kristan, W. B.; Kubiak, C. P.; Miller, E. W.; Tsien, R. Y., Improved PeT Molecules for Optically Sensing Voltage in Neurons. *Journal of the American Chemical Society* **2015,** *137* (5), 1817-1824.

7. Kulkarni, R. U.; Yin, H.; Pourmandi, N.; James, F.; Adil, M. M.; Schaffer, D. V.; Wang, Y.; Miller, E. W., A Rationally Designed, General Strategy for Membrane Orientation of Photoinduced Electron Transfer-Based Voltage-Sensitive Dyes. *ACS Chemical Biology* **2017,** *12* (2), 407-413.

8. Deal, P. E.; Kulkarni, R. U.; Al-Abdullatif, S. H.; Miller, E. W., Isomerically Pure Tetramethylrhodamine Voltage Reporters. *Journal of the American Chemical Society* **2016,** *138* (29), 9085-8.

9. Kulkarni, R. U.; Vandenberghe, M.; Thunemann, M.; James, F.; Andreassen, O. A.; Djurovic, S.; Devor, A.; Miller, E. W., In Vivo Two-Photon Voltage Imaging with Sulfonated Rhodamine Dyes. *ACS Central Science* **2018,** *4* (10), 1371-1378.

10. Huang, Y.-L.; Walker, A. S.; Miller, E. W., A Photostable Silicon Rhodamine Platform for Optical Voltage Sensing. *Journal of the American Chemical Society* **2015,** *137* (33), 10767-10776.

11. Kulkarni, R. U.; Kramer, D. J.; Pourmandi, N.; Karbasi, K.; Bateup, H. S.; Miller, E. W., Voltage-sensitive rhodol with enhanced two-photon brightness. *Proceedings of the National Academy of Sciences* **2017,** *114* (11), 2813-2818.

12. Kazemipour, A.; Novak, O.; Flickinger, D.; Marvin, J. S.; Abdelfattah, A. S.; King, J.; Borden, P. M.; Kim, J. J.; Al-Abdullatif, S. H.; Deal, P. E.; Miller, E. W.; Schreiter, E. R.; Druckmann, S.; Svoboda, K.; Looger, L. L.; Podgorski, K., Kilohertz frame-rate two-photon tomography. *Nature Methods* **2019,** *16* (8), 778-786.

13. Cajal, S., Estructura de los centros nerviosos de las aves. I. *Revist trimestr de Histol norm y patol* **1888,** *1*.

14. Glickstein, M., Golgi and Cajal: The neuron doctrine and the 100th anniversary of the 1906 Nobel Prize. *Current Biology* **2006,** *16* (5), R147-R151.

15. Golgi Stain. In *Encyclopedia of Neuroscience*, Binder, M. D.; Hirokawa, N.; Windhorst, U., Eds. Springer Berlin Heidelberg: Berlin, Heidelberg, 2009; pp 1756-1756.

16. Banghart, M.; Borges, K.; Isacoff, E.; Trauner, D.; Kramer, R. H., Light-activated ion channels for remote control of neuronal firing. *Nature Neuroscience* **2004,** *7* (12), 1381-1386.

17. Fortin, D. L.; Banghart, M. R.; Dunn, T. W.; Borges, K.; Wagenaar, D. A.; Gaudry, Q.; Karakossian, M. H.; Otis, T. S.; Kristan, W. B.; Trauner, D.; Kramer, R. H., Photochemical control of endogenous ion channels and cellular excitability. *Nature Methods* **2008,** *5* (4), 331-338.

18. Gubernator, N. G.; Zhang, H.; Staal, R. G. W.; Mosharov, E. V.; Pereira, D. B.; Yue, M.; Balsanek, V.; Vadola, P. A.; Mukherjee, B.; Edwards, R. H.; Sulzer, D.; Sames, D., Fluorescent False Neurotransmitters Visualize Dopamine Release from Individual Presynaptic Terminals. *Science* **2009,** *324* (5933), 1441-1444.

19. Sakamoto, S.; Yamaura, K.; Numata, T.; Harada, F.; Amaike, K.; Inoue, R.; Kiyonaka, S.; Hamachi, I., Construction of a Fluorescent Screening System of Allosteric Modulators for the GABAA Receptor Using a Turn-On Probe. *ACS Central Science* **2019,** *5* (9), 1541-1553.

20. Wakayama, S.; Kiyonaka, S.; Arai, I.; Kakegawa, W.; Matsuda, S.; Ibata, K.; Nemoto, Y. L.; Kusumi, A.; Yuzaki, M.; Hamachi, I., Chemical labelling for visualizing native AMPA receptors in live neurons. *Nature Communications* **2017,** *8* (1), 14850.

21. Grienberger, C.; Konnerth, A., Imaging Calcium in Neurons. *Neuron* **2012,** *73* (5), 862-885.

22. Farrants, H.; Hiblot, J.; Griss, R.; Johnsson, K., Rational Design and Applications of Semisynthetic Modular Biosensors: SNIFITs and LUCIDs. In *Synthetic Protein Switches: Methods and Protocols*, Stein, V., Ed. Springer New York: New York, NY, 2017; pp 101-117.

23. Chanda, B.; Blunck, R.; Faria, L. C.; Schweizer, F. E.; Mody, I.; Bezanilla, F., A hybrid approach to measuring electrical activity in genetically specified neurons. *Nature Neuroscience* **2005,** *8*, 1619.

24. Sjulson, L.; Miesenböck, G., Rational Optimization and Imaging In Vivo of a Genetically Encoded Optical Voltage Reporter. *The Journal of Neuroscience* **2008,** *28* (21), 5582-5593.

25. Xu, Y.; Peng, L.; Wang, S.; Wang, A.; Ma, R.; Zhou, Y.; Yang, J.; Sun, D.-e.; Lin, W.; Chen, X.; Zou, P., Hybrid Indicators for Fast and Sensitive Voltage Imaging. *Angewandte Chemie International Edition* **2018,** *57* (15), 3949-3953.

26. Abdelfattah, A. S.; Kawashima, T.; Singh, A.; Novak, O.; Liu, H.; Shuai, Y.; Huang, Y.-C.; Campagnola, L.; Seeman, S. C.; Yu, J.; Zheng, J.; Grimm, J. B.; Patel, R.; Friedrich, J.; Mensh, B. D.; Paninski, L.; Macklin, J. J.; Murphy, G. J.; Podgorski, K.; Lin, B.-J.; Chen, T.-W.; Turner, G. C.; Liu, Z.; Koyama, M.; Svoboda, K.; Ahrens, M. B.; Lavis, L. D.; Schreiter, E. R., Bright and photostable chemigenetic indicators for extended in vivo voltage imaging. *Science* **2019,** *365* (6454), 699-704.

27. Saminathan, A.; Devany, J.; Pillai, K. S.; Veetil, A. T.; Schwake, M.; Krishnan, Y., A DNA-based voltmeter for organelles. *bioRxiv* **2019**, 523019.

28. Ng, D. N.; Fromherz, P., Genetic Targeting of a Voltage-Sensitive Dye by Enzymatic Activation of Phosphonooxymethylammonium Derivative. *ACS Chemical Biology* **2011,** *6* (5), 444-451.

29. Grenier, V.; Walker, A. S.; Miller, E. W., A Small-Molecule Photoactivatable Optical Sensor of Transmembrane

Potential. *Journal of the American Chemical Society* **2015,** *137* (34), 10894-10897.

30. Liu, P.; Grenier, V.; Hong, W.; Muller, V. R.; Miller, E. W., Fluorogenic Targeting of Voltage-Sensitive Dyes to Neurons. *Journal of the American Chemical Society* **2017,** *139* (48), 17334-17340.

31. Ortiz, G.; Liu, P.; Naing, S. H. H.; Muller, V. R.; Miller, E. W., Synthesis of Sulfonated Carbofluoresceins for Voltage Imaging. *Journal of the American Chemical Society* **2019,** *141* (16), 6631-6638.

32. Sundukova, M.; Prifti, E.; Bucci, A.; Kirillova, K.; Serrao, J.; Reymond, L.; Umebayashi, M.; Hovius, R.; Riezman, H.; Johnsson, K.; Heppenstall, P. A., A Chemogenetic Approach for the Optical Monitoring of Voltage in Neurons. *Angewandte Chemie International Edition* **2019,** *58* (8), 2341-2344.

33. Grenier, V.; Daws, B. R.; Liu, P.; Miller, E. W., Spying on Neuronal Membrane Potential with Genetically Targetable Voltage Indicators. *Journal of the American Chemical Society* **2019,** *141* (3), 1349-1358.

34. Los, G. V.; Encell, L. P.; McDougall, M. G.; Hartzell, D. D.; Karassina, N.; Zimprich, C.; Wood, M. G.; Learish, R.; Ohana, R. F.; Urh, M.; Simpson, D.; Mendez, J.; Zimmerman, K.; Otto, P.; Vidugiris, G.; Zhu, J.; Darzins, A.; Klaubert, D. H.; Bulleit, R. F.; Wood, K. V., HaloTag: A Novel Protein Labeling Technology for Cell Imaging and Protein Analysis. *ACS Chemical Biology* **2008,** *3* (6), 373-382.

35. Shields, B. C.; Kahuno, E.; Kim, C.; Apostolides, P. F.; Brown, J.; Lindo, S.; Mensh, B. D.; Dudman, J. T.; Lavis, L. D.; Tadross, M. R., Deconstructing behavioral neuropharmacology with cellular specificity. *Science* **2017,** *356* (6333), eaaj2161.

36. Fang, X.; Fu, Y.; Long, M. J. C.; Haegele, J. A.; Ge, E. J.; Parvez, S.; Aye, Y., Temporally Controlled Targeting of 4-Hydroxynonenal to Specific Proteins in Living Cells. *Journal of the American Chemical Society* **2013,** *135* (39), 14496-14499.

37. Long, M. J. C.; Parvez, S.; Zhao, Y.; Surya, S. L.; Wang, Y.; Zhang, S.; Aye, Y., Akt3 is a privileged first responder in isozyme-specific electrophile response. *Nature Chemical Biology* **2017,** *13*, 333.

38. England, C. G.; Luo, H.; Cai, W., HaloTag Technology: A Versatile Platform for Biomedical Applications. *Bioconjugate Chemistry* **2015,** *26* (6), 975-986.

39. Zakeri, B.; Fierer, J. O.; Celik, E.; Chittock, E. C.; Schwarz-Linek, U.; Moy, V. T.; Howarth, M., Peptide tag forming a rapid covalent bond to a protein, through engineering a bacterial adhesin. *Proceedings of the National Academy of Sciences* **2012,** *109* (12), E690-E697.

40. Roubinet, B.; Bischoff, M.; Nizamov, S.; Yan, S.; Geisler, C.; Stoldt, S.; Mitronova, G. Y.; Belov, V. N.; Bossi, M. L.; Hell, S. W., Photoactivatable Rhodamine Spiroamides and Diazoketones Decorated with "Universal Hydrophilizer" or Hydroxyl Groups. *The Journal of Organic Chemistry* **2018,** *83* (12), 6466-6476.

41. Chesnut, J. D.; Baytan, A. R.; Russell, M.; Chang, M.-P.; Bernard, A.; Maxwell, I. H.; Hoeffler, J. P., Selective isolation of transiently transfected cells from a mammalian cell population with vectors expressing a membrane anchored single-chain antibody. *Journal of Immunological Methods* **1996,** *193* (1), 17-27.

42. Gronwald, R. G.; Grant, F. J.; Haldeman, B. A.; Hart, C. E.; O'Hara, P. J.; Hagen, F. S.; Ross, R.; Bowen-Pope, D. F.; Murray, M. J., Cloning and expression of a cDNA coding for the human platelet-derived growth factor receptor: evidence for more than one receptor class. *Proceedings of the National Academy of Sciences* **1988,** *85* (10), 3435-3439.

43. Medof, M. E.; Walter, E. I.; Roberts, W. L.; Haas, R.; Rosenberry, T. L., Decay accelerating factor of complement is anchored to cells by a C-terminal glycolipid. *Biochemistry* **1986,** *25* (22), 6740-6747.

44. Yang, Helen H.; St-Pierre, F.; Sun, X.; Ding, X.; Lin, Michael Z.; Clandinin, Thomas R., Subcellular Imaging of Voltage and Calcium Signals Reveals Neural Processing In Vivo. *Cell* **2016,** *166* (1), 245-257.

45. Shaner, N. C.; Lambert, G. G.; Chammas, A.; Ni, Y.; Cranfill, P. J.; Baird, M. A.; Sell, B. R.; Allen, J. R.; Day, R. N.; Israelsson, M.; Davidson, M. W.; Wang, J., A bright monomeric green fluorescent protein derived from Branchiostoma lanceolatum. *Nature Methods* **2013,** *10*, 407.

46. Sato, R.; Kozuka, J.; Ueda, M.; Mishima, R.; Kumagai, Y.; Yoshimura, A.; Minoshima, M.; Mizukami, S.; Kikuchi, K., Intracellular Protein-Labeling Probes for Multicolor Single-Molecule Imaging of Immune Receptor–Adaptor Molecular Dynamics. *Journal of the American Chemical Society* **2017,** *139* (48), 17397-17404.

47. Hori, Y.; Hirayama, S.; Sato, M.; Kikuchi, K., Redesign of a Fluorogenic Labeling System To Improve Surface Charge, Brightness, and Binding Kinetics for Imaging the Functional Localization of Bromodomains. *Angewandte Chemie International Edition* **2015,** *54* (48), 14368-14371.

48. Mizukami, S.; Watanabe, S.; Akimoto, Y.; Kikuchi, K., No-Wash Protein Labeling with Designed Fluorogenic Probes and Application to Real-Time Pulse-Chase Analysis. *Journal of the American Chemical Society* **2012,** *134* (3), 1623-1629.

49. Jing, C.; Cornish, V. W., A Fluorogenic TMP-Tag for High Signal-to-Background Intracellular Live Cell Imaging. *ACS Chemical Biology* **2013,** *8* (8), 1704-1712.

50. Schwartz, S. L.; Yan, Q.; Telmer, C. A.; Lidke, K. A.; Bruchez, M. P.; Lidke, D. S., Fluorogen-Activating Proteins Provide Tunable Labeling Densities for Tracking FcεRI Independent of IgE. *ACS Chemical Biology* **2015,** *10* (2), 539-546.

51. Keppler, A.; Gendreizig, S.; Gronemeyer, T.; Pick, H.; Vogel, H.; Johnsson, K., A general method for the covalent labeling of fusion proteins with small molecules in vivo. *Nature Biotechnology* **2003,** *21* (1), 86-89.

Rhodamine Voltage Reporter-HaloTag Hybrids

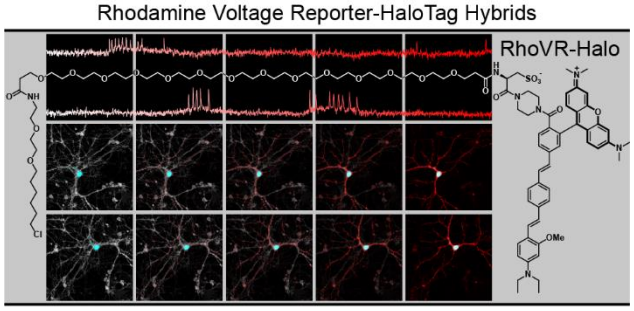

for genetically targeted voltage imaging in neurons